Protein Repellency of Well-Defined, Concentrated Poly(2-hydroxyethyl methacrylate) Brushes by the Size-Exclusion Effect

Chiaki Yoshikawa,[†] Atsushi Goto,[†] Yoshinobu Tsujii,[†] Takeshi Fukuda,*[,†] Tsuyoshi Kimura,[§] Kazuya Yamamoto,[‡] and Akio Kishida[§]

Institute for Chemical Research, Kyoto University, Uji, Kyoto 611-0011, Japan; Department of Nanostructured and Advanced Materials, Graduate School of Science and Engineering, Kagoshima University, 1-21140 Korimoto, Kagoshima 890-0065, Japan; and Institute of Biomaterials and Bioengineering, Tokyo Medical and Dental University, Chiyoda, Tokyo 101-0062, Japan

Received September 17, 2005; Revised Manuscript Received November 10, 2005

ABSTRACT: The adsorption of proteins on poly(2-hydroxyethyl methacrylate) (PHEMA) brushes was systematically studied by quartz crystal microbalance (QCM) and fluorescence microscopy as a function of graft density and protein size. The graft density σ (chains/nm^2) ranged from 0.007 (dilute or semidilute brush regime) to 0.7 (concentrated brush regime), and the protein size ranged from 2 to 13 nm in an effective diameter. The lowest-density brush ($\sigma = 0.007$) adsorbed all the tested four proteins, while the highest-density brush ($\sigma = 0.7$) adsorbed none of them. The middle-density brush ($\sigma = 0.06$) showed an intermediate behavior, adsorbing the smallest two proteins but effectively repelling the largest two. PHEMA cast films adsorbed a probe protein with the adsorbed amount increasing approximately proportionally to the film thickness, indicating that the adsorption mainly occurred in the bulk of the film. The noted results for the brushes support the idea of size-exclusion effect, an effect characteristic of concentrated polymer brushes, in which the graft chains are highly extended and highly oriented so that large molecules, sufficiently large compared with the distance between the nearest-neighbor graft points, are *physically* excluded from the entire brush layer. In this regard, the behavior of the lowest-density brush should be essentially similar to that of the cast film, as was in fact observed.

Introduction

Living radical polymerization (LRP) has been applied to surface-initiated graft polymerization, allowing controlled grafting of well-defined polymers from various solid surfaces with dramatically high surface densities.[1−9] The surface density σ reached as large as 0.7 chains/nm^2 for common polymers like poly(methyl methacrylate) (PMMA) and polystyrene (PS).[9] This density was more than 1 order of magnitude higher than those of typical "semidilute" brushes, going deep into the "concentrated brush" regime which had been little explored systematically because of the unavailability of such brush samples. Recent studies revealed that these concentrated brushes have structure and properties quite different and even unpredictable from those of semidilute brushes:[9] most strikingly, the PMMA concentrated brushes swollen in a good solvent (toluene) exhibited an equilibrium film thickness as large as 80−90% of the full (contour) length of the graft chains, indicating that the chains are extended to a similarly high degree.[9,10] The surface density of 0.7 chains/nm^2 for a PMMA brush, for example, also means that the thickness of the dry film reaches about 40% of the full length of the chains, which is much larger than the mean size of the chains in a random-coil (or so-called "mushroom") conformation. Presumably reflecting this characteristic conformational feature of concentrated brushes, dry PMMA brushes had a glass transition temperature significantly higher,[11] and a plate compressibility markedly smaller,[12] than those of the equivalent cast films. More interestingly, they were immiscible even with free PMMA of an oligomeric chain length.[9,13] This last observation suggests that concentrated brushes in the melt have a size-exclusion effect of (conformational) entropic origin. A similar effect is expectable for concentrated brushes swollen in a good solvent, as, in fact, was demonstrated chromatographically by using the silica monolith column coated with concentrated PMMA brushes.[9,14]

As one of the most interesting potential applications of polymer brushes, attention has been directed toward biointerfaces to tune interactions of solid surfaces with biologically important materials. For example, proteins will adsorb on surfaces through nonspecific interactions, often triggering a biofouling, e.g., the deposition of biological cells, bacteria, and so on. Attempts have been made to modify surfaces with polymer brushes to prevent protein adsorption. To understand the process of protein adsorption, the interactions between proteins and brush-coated surfaces can be modeled by the three generic modes illustrated in Scheme 1a (after Curie et al.[15] with some modifications). One is the primary adsorption, in which a protein diffuses into the brush and adsorbs on the substrate surface. The secondary adsorption is the one occurring at the outermost surface of the swollen brush film. The last one is the tertiary adsorption, which is caused by the interaction of protein with the polymer segments within the brush layer. For relatively small proteins, the primary and tertiary adsorptions would be particularly important, but they should become less important with increasing protein size and increasing graft density, since a larger protein would be more difficult to diffuse against the concentration gradient formed by the polymer brush, and this gradient, clearly, is a function of graft density. However, the size and density dependence of protein adsorption would manifest itself much more clearly for concentrated brushes due to a different mechanism. As already noted, the graft chains in

[†] Kyoto University.
[‡] Kagoshima University.
[§] Tokyo Medical and Dental University.
* Corresponding author: e-mail fukuda@scl.kyoto-u.ac.jp.

10.1021/ma0520242 CCC: $33.50
Published on Web 02/25/2006

Scheme 1. Schematic Illustration of (a) Possible Interactions of Probe Molecules with a Polymer Brush and (b) Size-Exclusion Effect of Concentrated Brush

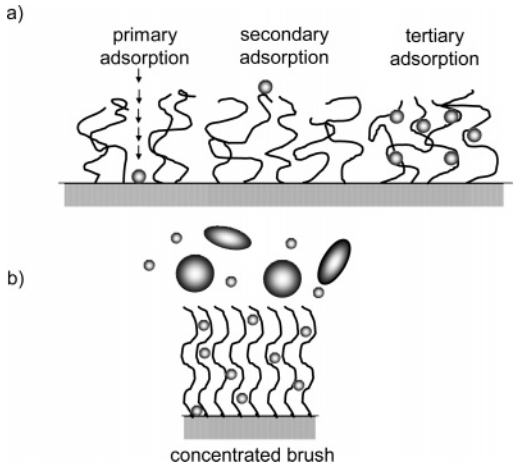

a concentrated brush are highly extended and hence highly oriented so that the entire brush layer, from the substrate surface to the outermost surface throughout, could have a size-exclusion effect (Scheme 1b). By the terms "size exclusion", we stress the *physical* aspect of the phenomenon, meaning that the protein (or probe molecule) is excluded from the brush layer to avoid the large (mainly conformational) entropy loss caused on the highly extended chains by the entrance of the large molecule. Since the degree of chain extension is much less significant in semidilute brushes, this effect should be minor for them.

In the past, poly(ethylene oxide) (PEO)-grafted surfaces were extensively studied to discuss their protein adsorption behavior as a function of graft density.[15−21] However, since those surfaces were prepared by physisorption of block copolymers or comb-like polymers using a self-assembling or the Langmuir−Blodgett technique, the graft density should have been in a semidilute regime, i.e., too low to observe the mentioned effect clearly, if any present. Well-defined concentrated brushes achievable by surface-initiated LRP would set up size-exclusion limits at much smaller sizes of probe molecules, thus allowing us to explore them with available proteins. Most recently, poly(acrylamide),[22] poly(2-(dimethylamino)ethyl methacrylate),[23] poly(oligo(ethylene glycol) methyl methacrylate),[24] and poly(2-methacryloxyethylphosphorylcholine) (PMPC)[25−27] brushes were prepared by surface-initiated LRP and observed to show good adsorption resistance for proteins and cells. From a mechanistic point of view, however, these studies remained purely qualitative, paying little attention to the mentioned characteristics of concentrated brushes.

In this work, we have attempted to substantiate the postulated size-exclusion effect of concentrated polymer brushes by systematically studying the adsorption behavior of varying sizes of proteins on the substrates grafted with a poly(2-hydroxyethyl methacrylate) (PHEMA) brush of varying surface densities, by means of quartz crystal microbalance (QCM) and fluorescence microscopy. PHEMA is a hydrophilic, biocompatible polymer,[28] but the biocompatibility of PHEMA cast film is reported to be not as good as e.g. PMPC[29,30] and poly(2-methoxyethyl acrylate) cast films.[31,32] Hence, any favorable results that PHEMA brushes may present could be ascribed more to the structural, rather than thermodynamic, properties of the system. Our ultimate goal is to develop, by utilizing the advantages of surface-initiated LRP,[9] a concentrated brush-based, new biointerface that will completely suppress the adsorption of small as well as large proteins. This work should be an important step for this goal.

Scheme 2. Schematic Illustration of Graft Polymerizations on an Inorganic Substrate: (a) Surface-Initiated ATRP and (b) a Grafting-To Method

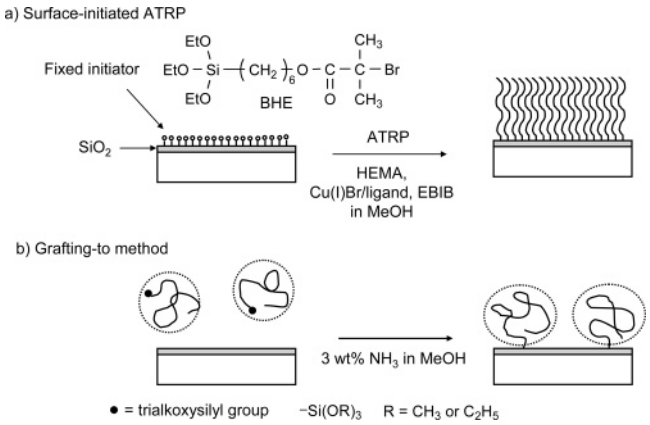

Experimental Section

Materials. 2-Hydroxyethyl methacrylate (HEMA) (99%, Nacalai Tesque, Japan) was purified according to the literature.[33] Cu(I)Br (99.9%, Wako Pure Chemical, Japan), ethyl 2-bromoisobutylate (EBIB) (99%, Wako), 2,2-bipyridine (bpy) (99%, Nacalai), methanol (99%, Nacalai), phosphate-buffered saline (PBS) (pH = 7.4, Wako), ammonia (28% aqueous, Nacalai), 3-mercaptopropyltrimethoxysilane (S810) (Chisso, Japan), and 2,2′-azobis(4-methoxy-2,4-dimethylvaleronitrile) (V70) (99.9%, Wako) were used as received. 6-(2-Bromo-2-isobutyloxy)hexyltriethoxysilane (BHE), a fixable initiator for ATRP, was prepared, as previously reported.[34] Bovine serum aprotinin (Aprotinin), bovine serum albumin (BSA), fluorescein isothiocyanate-labeled BSA (FITC-BSA), bovine serum immunoglobulin G (IgG), and horse heart myoglobin (Myoglobin) were purchased from Sigma-Aldrich and used as received.

Silicon wafers were cleaned by ultrasonication in $CHCl_3$ for 30 min and ultraviolet (UV)/ozone treatment for 10 min. The UV/ozone treatment effectively removed organic contaminants on the wafer surfaces. QCM chips (optically polished square-shaped AT-cut quartz crystals (1×1 cm^2) with gold electrodes) (Seiko EG&G, Seiko Instruments Inc.) were similarly cleaned. On the cleaned chip, Cr and then SiO_2 were deposited in a vacuum with the thicknesses of 5 and 40 nm, respectively.

Preparation of High-Density Brushes (σ = 0.7 Chains/nm^2). High-density PHEMA brushes were prepared by surface-initiated ATRP, as shown in Scheme 2a. A silicon wafer and a SiO_2-deposited QCM chip were immersed in a tetrahydrofuran (THF) solution of BHE (1 wt %) and NH_3 (1 wt %) for 12 h at room temperature and washed with THF. The BHE-immobilized substrate (wafer and chip) was immersed in a degassed methanol solution of HEMA (4.5 M), Cu(I)Br (25 mM), bpy (63 mM), and the free initiator EBIB (22.5 mM), sealed under vacuum in a glass tube (1 cm diameter), and heated at 40 °C for a prescribed time. This polymerization condition was referred to Armes et al., who successfully prepared low-polydispersity free polymers of HEMA.[35] After polymerization, the solution was diluted with *N*,*N*-dimethylformamide (DMF) to a known concentration and analyzed by gel permeation chromatography (GPC). The conversion was determined from the GPC peak area. The substrate was rinsed in a Soxhlet apparatus with methanol for 5 h to remove physisorbed free polymers and impurities.

Preparation of Middle- and Low-Density Brushes (σ = 0.06 and 0.007 Chains/nm^2). Middle- and low-density PHEMA brushes were prepared by a grafting-to method, as shown in Scheme 2b. Namely, PHEMA chains with an alkoxysilyl group at one chain end were immobilized on a silicon wafer and a SiO_2-deposited QCM chip in solution. Two end-functionalized PHEMAs with different chain lengths were used. The shorter one (M_n = 9800 and M_w/M_n = 1.2) was synthesized by ATRP with BHE (with a triethoxysilyl group) used as a free initiator: a degassed methanol solution of HEMA (4.5 M), BHE (22.5 mM), Cu(I)Br (25 mM), and bpy (63

Table 1. Characteristics of Studied PHEMA Surfaces

surface[a]	$M_{n,conv}$[b]	$M_{n,PEG}$[c]	M_w/M_n[c]	L[d]/(nm)	σ[e]/(chain nm^{-2})	d[f]/(nm)	θ[g]/(deg)
high-density brush	1700	3500	1.21	2	0.7	1	29
high-density brush	9700	8000	1.26	10	0.7	1	
high-density brush	16800[h]	12300	1.30	15	0.7	1	29
middle-density brush	19000	15300	1.27	2	0.06	4	27
low-density brush		1.2×10^5	1.24	2	0.007[i]	12	29
cast film		$>4 \times 10^5$		30			23
cast film		$>4 \times 10^5$		90			23
cast film		$>4 \times 10^5$		330			23
BHE[j]							55

[a] Characteristics of brushes were almost identical on silicon wafers and QCM chips, and typical values on silicon wafers are listed. [b] Calculated according to eq 3. [c] Estimated by PEG-calibrated GPC. [d] Film thickness, the error is within 10%. [e] Graft density, calculated with L and $M_{n,conv}$ according to eq 2. [f] Average distance between the nearest-neighbor graft points, calculated according to $d = \sigma^{-1/2}$. [g] Contact angle; the error is within 2°. [h] The $M_{n,MALLS}$ is 17600 (see text). [i] Calculated with L and $M_{n,MALLS}$ (1.8×10^5) according to eq 2. [j] BHE-immobilized surface.

mM) was heated at 30 °C for 1 h. After reprecipitation with cooled water, there was isolated a PHEMA ($M_n = 1.5 \times 10^4$ and $M_w/M_n = 1.2$) possessing a triethoxysilyl group (derived from BHE) at one chain end. A silicon wafer and a SiO_2-deposited QCM chip were immersed in a methanol solution of the PHEMA (1 wt %) and NH_3 (2 wt %) for 12 h at room temperature and rinsed in a Soxhlet apparatus with methanol for 5 h, yielding a middle-density brush ($\sigma = 0.06$ chains/nm^2).

The longer end-functionalized PHEMA was prepared by the conventional radical polymerization with the chain transfer agent S810: a methanol solution of HEMA (4.5 M), S810 (chain transfer agent; 9 mM), and V70 (9 mM) was heated at 40 °C for 2 h. The obtained polymer was fractionated by use of a preparative GPC, yielding a PHEMA ($M_n = 1.2 \times 10^5$ and $M_w/M_n = 1.2$) possessing a trimethoxysilyl group (derived from S810) at one chain end. This polymer was immobilized on a silicon wafer and a SiO_2-deposited QCM chip as described above, yielding a low-density brush ($\sigma =$ 0.007 chains/nm^2).

Preparation of Cast Films. PHEMA ($M_v = 10^6$) (Aldrich), after having purified by reprecipitation from a methalol solution into cold water, was dissolved in methanol. The cast films were obtained by spin-casting the PHEMA solution onto a silicon wafer using a homemade spin-coater at a spinning speed of 2000 rpm for 2 min, followed by annealing at 80 °C for 24 h in a vacuum. The film thickness was controlled by changing the concentration of PHEMA solution.

QCM Measurement. Protein adsorption was studied at 25 °C with a quartz crystal analyzer 917 (Seiko EG&G) driving a 9 MHz QCM chip. The QCM chip was mounted in a thermostated homemade QCM cell by means of O-ring seals, which allowed only one face of the chip to come in contact with the solution. Before injection of a PBS solution of a protein, the QCM cell was initially filled with PBS and rinsed several times until a stable baseline was established. The stability of the frequency of QCM was ±0.3 Hz within 1 h at 25 °C in water. The adsorbed amount Δm (ng) is represented by[36]

$$\Delta m = -\Delta f A((\mu_q \rho_q)/(2F_q^2))^{1/2} \quad (1)$$

where Δf is the frequency change (Hz), F_q is the parent frequency of QCM (9 MHz), μ_q is the shear modules of quartz (2.947×10^{11} g/(cm s^2)), ρ_q is the density of quartz (2.648 g/cm^3), and A is the surface area of electrode (0.196 cm^2).

Fluorescence Microscopic Observation. The sample was immersed in a PBS solution of FITC-BSA (1.0 g/L) for a prescribed time at room temperature. The sample was washed by softly immersing in PBS, and this procedure was repeated five times with fresh PBS. Fluorescence images were taken on an optical microscope (Eclipse TE2000, Nikon, Tokyo, Japan) equipped with a highly sensitive CCD camera (ORCA-ER, Hamamatsu Photonics, Shizuoka, Japan). The observation was made on at least five spots for each sample, and the fluorescence intensities of these spots were averaged. To check reproducibility of the FITC-BSA adsorption, at least three samples were prepared under the same conditions and examined.

Other Measurements. The GPC analysis for PHEMA was made on a Tosoh CCP&8020 series high-speed liquid chromatograph (Tokyo, Japan) equipped with two Shodex gel columns LF804 (300 × 80 mm; bead size = 6 μm; pore size = 20−3000 Å) (Tokyo). DMF was used as eluent with a flow rate of 0.8 mL/min (40 °C). The column system was calibrated with Tosoh standard poly(ethylene glycol)s (PEGs). Sample detection and quantification were made with a Tosoh differential refractometer RI-8020. Sample detection was also made with a multiangle laser light scattering (MALLS) detector, a Wyatt Technology DAWN EOS (Santa Barbara, CA), equipped with a Ga−As laser ($\lambda = 690$ nm). The refractive index increment dn/dc was determined to be 0.075 mL g^{-1} by a Wyatt Technology OPTILAB DSP differential refractometer ($\lambda = 690$ nm).

For the GPC analysis of proteins, the above-noted chromatograph equipped with a Shodex gel column KW804 (300 × 80 mm; bead size = 7 μm; pore size = 300 Å) (Tokyo) was calibrated with Shodex standard pullulans. PBS was used as eluent with a flow rate of 0.8 mL/min (30 °C).

The fractionation of PHEMA was made on a preparative LC-918 liquid chromatograph (Japan Analytical Industry, Tokyo) equipped with JAIGEL GS-510 poly(vinyl alcohol) gel columns (500 × 21.5 mm; bead size = 16 μm). Methanol was used as eluent with a flow rate of 5.0 mL/min (room temperature).

The thicknesses of the deposited Cr and SiO_2 and the grafted and spin-casted PHEMA layers were determined by a compensator-rotating, spectroscopic ellipsometer (M-2000U, J.A. Woolam, Lincoln, NE) equipped with D_2 and QTH lamps. The polarizer angle was 45°, and the incident angles were 60°, 65°, and 70°. From the ellipsometric data, the thickness of PHEMA layer was evaluated using the optical constants determined for the spin-cast layer with a thickness of ca. 200 nm. The graft density σ was estimated from

$$\sigma = L\rho N_A/M_n \quad (2)$$

where L is the thickness of graft layer, ρ is the bulk density of PHEMA (1.15 g/cm^3), N_A is the Avogadro number, and M_n is the number-average molecular weight.

Contact angles (θ) were measured at room temperature with a contact angle meter CA-X (Kyowa Interface Science, Saitama, Japan). The measurement was made on at least five spots for each sample, and these θ values were averaged.

Results and Discussion

Preparation and Characterization of PHEMA Brushes. The "high-density" PHEMA brushes were prepared by surface-initiated ATRP. A few previous reports dealt with surface-initiated LRP of HEMA,[37−39] but we made an independent effort to optimize polymerization conditions to meet our purpose. Three samples with different chain lengths of PHEMA (and hence, different thicknesses of the graft layer) were prepared by varying the polymerization time. Table 1 lists the M_n and M_w/M_n of the free polymers simultaneously produced from the free initiator in the solution. These values can be used as

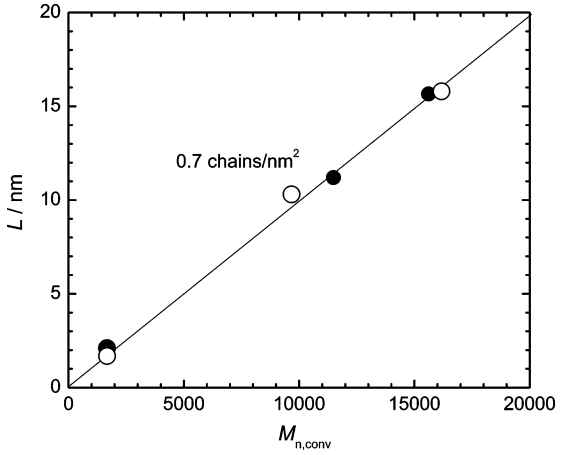

Figure 1. Plot of L vs $M_{n,conv}$ for the high-density brushes prepared on (●) silicon wafer and (○) QCM chip.

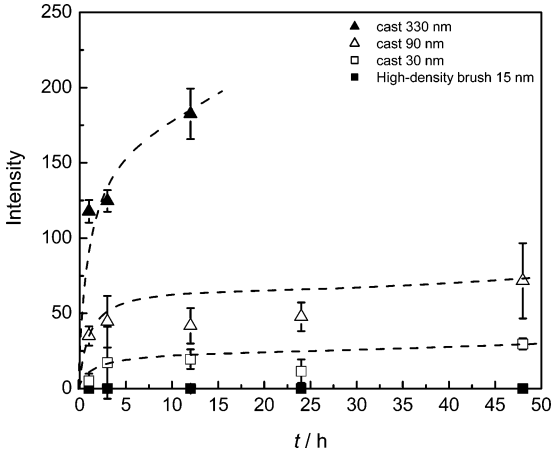

Figure 2. Plot of fluorescence intensity of adsorbed FITC-BSA vs soaked time t (25 °C) for the cast films with L = (▲) 330 nm, (△) 90 nm, and (□) 30 nm and the high-density brush with L = 15 nm (■). The FITC-BSA concentration was 1.0 g/L.

sufficiently accurate indices for those of the graft polymers.[4] The M_w/M_n was 1.2−1.3 in all cases, suggesting a well-controlled polymerization. The $M_{n,conv}$ was calculated using the following equation:

$$M_{n,conv} = [HEMA]_0/[EBIB]_0 \times MW \times C/100 \qquad (3)$$

where $[HEMA]_0$ and $[EBIB]_0$ are the feed concentration of HEMA and EBIB, respectively, MW is the molecular weight of HEMA, and C is the monomer conversion in percent. This value is the theoretical M_n for an ideal living polymerization. To evaluate the absolute value of M_n, the GPC detection was made with a MALLS detector for the highest-molecular-weight sample (prepared by the ATRP): the thus-determined M_n ($M_{n,MALLS}$ = 17 600) agreed well with the theoretical value ($M_{n,conv}$ = 16 800) rather than the PEG-calibrated M_n ($M_{n,PEG}$ = 12 300). For the oligomeric PHEMAs prepared by nearly the same ATRP system, Armes et al. reported that the absolute M_n determined by NMR was approximately equal to the $M_{n,conv}$.[35] We will use $M_{n,conv}$ for the absolute value.

The thickness L of the graft layer measured by ellipsometry linearly increased with increasing $M_{n,conv}$ of the free polymer (see Figure 1), suggesting a uniform growth of graft polymer with a constant surface density. From the slope of the line in Figure 1, the graft density σ was estimated to be ca. 0.7 chains/nm^2, which is similar to the highest values reported for PMMA and PS brushes.[9] Brushes with lower graft densities were prepared by a grafting-to method using two end-functionalized PHEMAs with $M_n = 1.5 \times 10^4$ and 1.2×10^5. They gave the "middle-density" (σ = 0.06 chains/nm^2) and "low-density" (σ = 0.007 chains/nm^2) brushes, respectively. These PHEMA brushes can be grouped into two series: one series is the high-density brushes with a nearly constant graft density of 0.7 chains/nm^2 and different dry film thicknesses 2, 10, and 15 nm, and the other is the brushes with nearly the same dry film thickness of 2 nm and different graft densities 0.007, 0.06, and 0.7 chains/nm^2.

The contact angle θ was measured in water by the air-bubble method for these brushes as well as a BHE-immobilized wafer and three PHEMA spin-cast films of thicknesses 30, 90, and 330 nm (Table 1). The BHE-immobilized surface (nongrafted surface) was much more hydrophobic than the PHEMA-coated samples (brushes and cast films). The brushes had a θ value slightly (about 5°) higher than the cast films (the experimental error in θ was ±2°), for an unclear reason. The observed dependence (or independence) of θ on graft density and film thickness suggests that the substrate was completely covered with PHEMA segments in all cases. The effect of the chain end (bromine for the high- and middle-density brushes and hydrogen for the low-density brush) is not evident even for the high-density brushes, in which, because of their oriented structure stressed above, the free chain ends and hence the bromine groups should be populated in the outermost surface of the film.

Adsorption of BSA. By fluorescence microscopy, we examined the adsorption of BSA on PHEMA cast film as a function of thickness: the cast films with different thicknesses (L = 30, 90, and 330 nm) prepared on silicon wafers were soaked in a FITC-BSA solution (1 g/L) at room temperature for a prescribed time, rinsed with PBS, and then observed by a fluorescence microscope. The fluorescence intensity was almost unchanged by further rinsing with PBS, confirming an irreversible adsorption. The fluorescence images suggested that BSA was homogeneously adsorbed (in an optical microscopic scale). Figure 2 shows the plot of fluorescence intensity vs soaked time. Unfortunately, the fluorescence intensity was not calibrated to the amount of adsorbed BSA, but the proportional relationship between them may reasonably be assumed. As a rough measure of the adsorbed amount, we may refer to the previous study reporting that 0.38 μg/cm^2 of BSA was adsorbed on PHEMA cast films.[32] The fluorescence intensity and hence the amount of adsorbed BSA gradually increased in several hours, approaching a constant (saturation) value. As Figure 3 shows, the intensity at 12 h, as a measure of the saturation value, increased almost proportionally to film thickness L. This means that BSA diffuses deeply into the bulk of the cast film, and that the adsorption in this system consists mainly of the tertiary adsorption with minor contributions of the primary and secondary ones. It naturally took a very long time to reach the saturation value (as compared with the case of high-density brush samples, for example, to be described below).

Next, we examined the adsorption of BSA on the brushes and the BHE-immobilized surfaces by QCM. This method allows in situ monitoring of the adsorption process with a usually high sensitivity. However, when it is applied to a viscoelastic layer in solution, the dissipation effect causes an error in estimating the mass according to eq 1. This error becomes larger with increasing layer thickness, and for this reason, our cast films were too thick to apply QCM. We confirmed that the QCMs with different fundamental frequencies (5 and 9 MHz) gave a consistent result for the brush samples with L = 10 nm or thinner, meaning that the dissipation effect was minor for

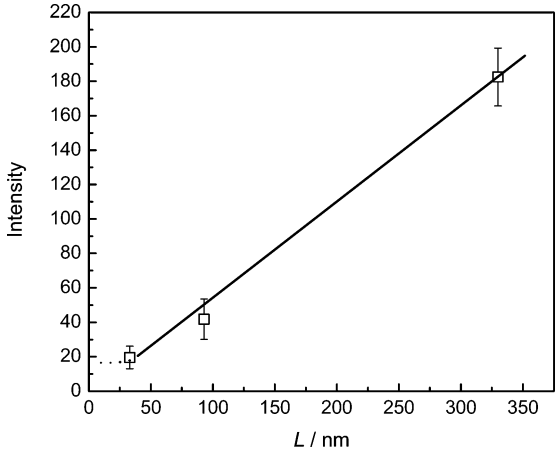

Figure 3. Plot of intensity of adsorbed FITC-BSA vs L for the cast films soaked for 12 h (25 °C). The FITC-BSA concentration was 1.0 g/L.

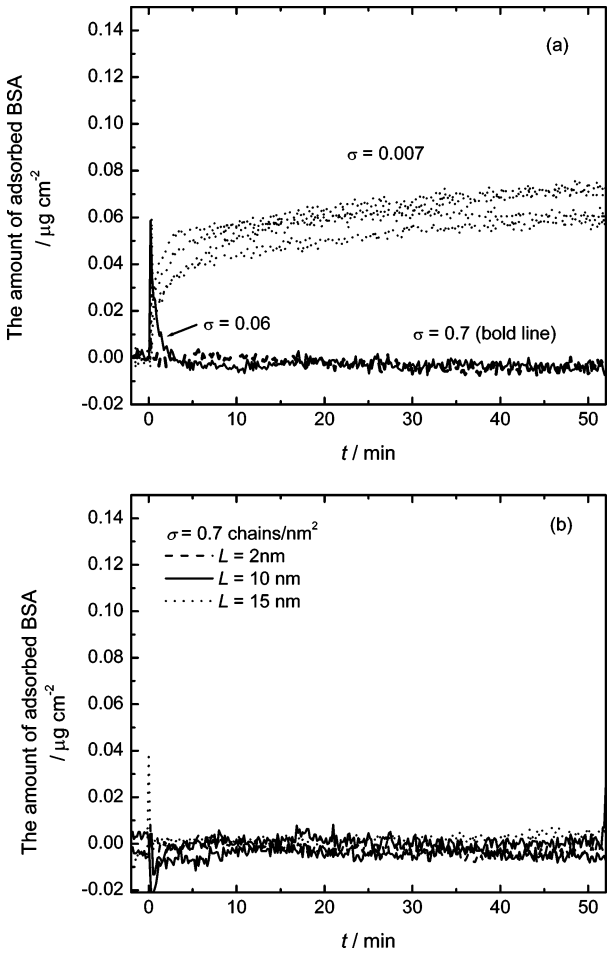

Figure 4. Time evolution of the amount of adsorbed BSA (25 °C) on (a) PHEMA brushes (σ = 0.007, 0.06, and 0.7 chains/nm^2) with L = 2 nm and (b) high-density PHEMA brushes (σ = 0.7 chains/nm^2) with L = 2, 10, and 15 nm. The BSA concentration was 1.0 g/L.

them. Figure 4 shows the results of the QCM measurement (25 °C) at an early stage of adsorption (<1 h), where the concentration of BSA in solution was 1 g/L. The adsorbed amount of BSA given in the ordinate axis was calculated from the frequency change according to eq 1. A sharp peak appearing, in some cases, immediately after the injection of BSA is due to the slight change in pressure and/or temperature on injection. The amount of BSA adsorbed onto the BHE-immobilized surface was 0.28 μg/cm^2 at 1 h (the data not shown), which is close to the value (0.25 μg/cm^2) reported for the side-on monolayer adsorption of BSA.[40] To confirm reproducibility of the measurement, we conducted at least five runs for each sample (an example is given for the low-density brush in Figure 4a, suggesting an experimental error of ±10%). BSA was readily (within 10 min) adsorbed on the low-density brush as well as the BHE surface and not desorbed by washing with PBS, indicating an irreversible adsorption. The amount of BSA adsorbed on the low-density brush at 1 h was ca. 0.07 μg/cm^2 (see Figure 4a), which is smaller than that for the BHE surface but still significant. On the other hand, there was no detectable adsorption on the middle- and high-density brushes (Figure 4a) with L = 2 nm. Figure 4b also shows that the high-density brushes with different thicknesses (L = 2, 10, and 15 nm) were all free from adsorption. These data clearly demonstrate that, by increasing the graft density, the adsorption of BSA can be suppressed. BSA has an ellipsoidal shape with an approximate dimension of 3 × 8 × 9 nm^3,[40−43] while the average distance d ($= \sigma^{-1/2}$) between the nearest-neighbor graft points is approximately 12, 4, and 1 nm for σ = 0.007, 0.06, and 0.7 chains/nm^2, respectively (Table 1). This reasonably suggests that BSA is difficult to diffuse into the swollen layer of the middle- and high-density brushes, on which no adsorption of BSA was, in fact, observed. The longer-term stability of protein repellency on the high-density brushes was studied by fluorescence microscopy, for the QCM experiment was difficult due to a baseline drift: no adsorption of FITC-BSA was detected on them even after 2 days.

Table 2. Absolute and Pullulan-Calibrated Molecular Weights, Crystallographic Dimensions, and $2R_g$ for Studied Proteins

protein	mol wt M	pullulan-calibrated M	crystallographic dimensions/nm	$2R_g$[a]/ nm
Aprotinin	6 500	1 500		2
Myoglobin	17 000	5 900	3 × 4 × 4	4
BSA	67 000	22 800	3 × 8 × 9	10
IgG	146 000	35 000		13

[a] Calculated (see text).

Adsorption of Proteins with Different Sizes. QCM experiments were conducted with the brush samples for a series of proteins with different sizes: Aprotinin (molecular weight = 6500), Myoglobin (17 000), BSA (67 000), and IgG (146 000). The characteristics of the four proteins are listed in Table 2. As the size of protein, crystallographic data are available for Myoglobin and BSA but not for the other two. The apparent molecular weights of these four proteins estimated by pullulan-calibrated GPC were 1500, 5900, 23 000, and 35 000 for Aprotinin, Myoglobin, BSA, and IgG, respectively, from which their radii of gyration (R_g) were estimated to be 1, 2, 5, and 6.5 nm, respectively, by using the known relation[44,45] between the R_g and molecular weight of pullulan. As shown in Table 2, the values of $2R_g$ may be good indices for the protein size (compare these values with the crystallographically determined dimensions of Myoglobin and BSA).

Figure 5 shows the amount of adsorbed protein after 1 h of soaking. The low-density brush adsorbed all the proteins, the middle-density one adsorbed only Aprotinin and Myoglobin, and the high-density one adsorbed none. These data show a clear dependence of adsorption on protein size and brush density: very crudely, we can state that no significant adsorption of protein takes place on a PHEMA brush when the brush d is smaller than the protein $2R_g$.

All these results confirm the size-exclusion effect of concentrated brushes. This effect would reduce the primary and tertiary adsorptions but not necessarily the secondary adsorption.

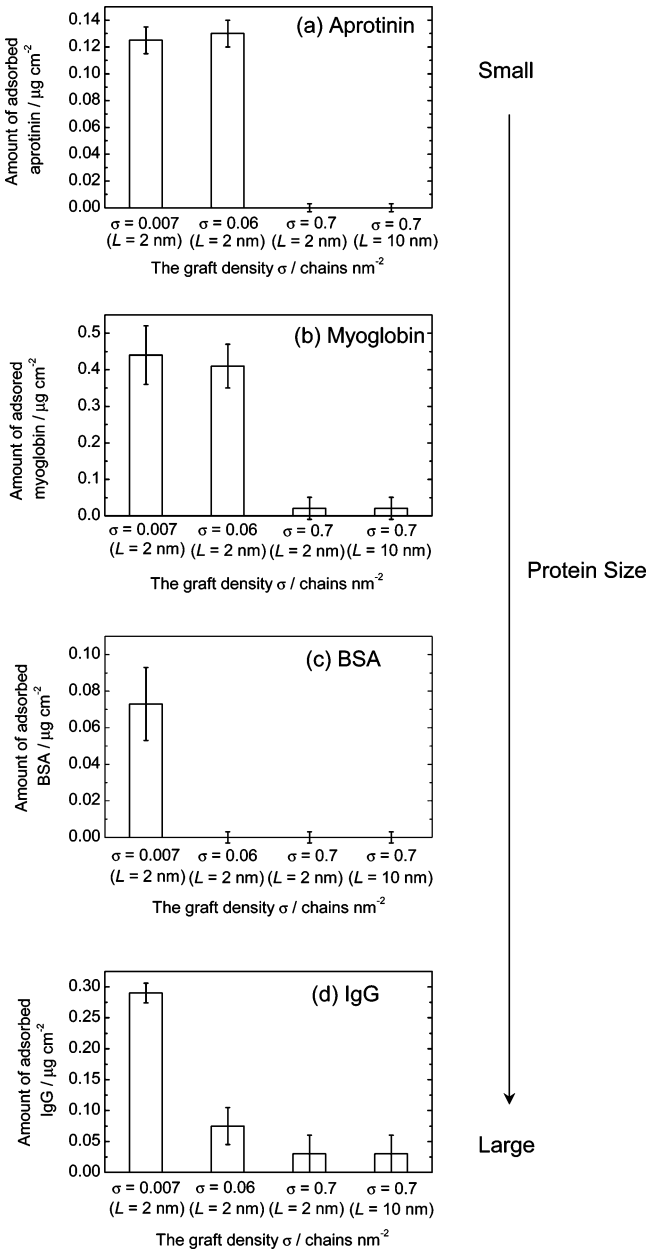

Figure 5. Amounts of adsorbed proteins onto PHEMA brush surfaces, soaked for 1 h (25 °C): (a) Aprotinin, (b) Myoglobin, (c) BSA, and (d) IgG. The protein concentration was 1.0 g/L in all cases.

The secondary adsorption can be induced by two possible interactions: one is the van der Waals and/or Coulombic interaction between the protein and the substrate, which should depend on the thickness of the brush layer.[15] The other is the interaction between the protein and the brush itself (at its outermost surface). The latter possibly depends on e.g. the water content of the brush layer,[46] the mobility of the brush chain,[47] and the structure of water near the brush surface.[31,32] Even though these details remain to be explored, the fact that no significant adsorption of any protein was detected on the high-density PHEMA brush indicates that the secondary adsorption is unimportant for this brush and these proteins. Figure 5 may indicate a nonnegligible adsorption of IgG on the high-density brush, but this may be ascribed to the insufficient number of trials, since another type of independent test (not shown here), which consisted of cycles of protein injection and rinsing, gave no indication of adsorption of this and other proteins on the high-density brush. To be stressed is the above-noted fact that the high-density brushes of different thickness repelled a protein (BSA) equally effectively. This means, on one hand, that no thick brush is needed for this purpose and, on the other hand, that a thick brush has a size-exclusion effect from its bottom to the outer surfaces through out. This is the very feature expected for a concentrated brush.

Finally, a comment is due regarding the block copolymer of PHEMA-PS type. Even though PHEMA cast films themselves have rather poor biocompatibility, as we have observed for the protein repellency, PHEMA-PS block copolymers are known to show improved biocompatibility.[48,49] At first, this improved biocompatibility was considered to have something to do with a microdomain surface structure caused by the phase separation of the PHEMA and PS segments. However, the ground for this interpretation seemed to have been lost, when the later structural studies on the cast films of these block copolymers revealed that the outermost surface of the films in water was preferentially covered with the laterally phase-separated PHEMA layer.[50−52] On the basis of our results, we would suggest the formulation of a concentrated brushlike structure of the PHEMA layer, in which the PHEMA chains are extruding out into the water phase from the hydrophobic (unswollen) PS layer, thereby repelling proteins or other large molecules by a size-exclusion effect.

Conclusions

The cast films and low-density brush ($\sigma = 0.007$ chains/nm^2) of PHEMA showed poor resistance against protein adsorption, which was reasonably ascribed to the tertiary adsorption, i.e., the adsorption induced by the interaction within the bulk of the PHEMA layer. On the other hand, the high-density brush ($\sigma = 0.7$ chains/nm^2) showed excellent resistance even for a protein as small as Aprotinin, independently of the brush thickness ($L = 2-15$ nm). The middle-density brush showed an intermediate behavior, adsorbing smaller proteins but effectively repelling larger proteins. There was a good correlation between the protein size and the threshold graft density beyond which the protein does not adsorb. (The secondary adsorption, occurring on the outermost surface of the PHEMA brushes, was inherently weak for the studied proteins.) These results confirmed the idea of size-exclusion effect of concentrated brushes. In general, it is suggested that the surface adsorption of large molecules like proteins can be greatly suppressed by densely grafting a polymer, i.e., controlling the *physical structure* of the polymer layer. With other unique properties of concentrated polymer brushes along with a range of possibility to design chain architecture by LRP, PHEMA concentrated brushes will find a wide variety of applications as a novel biointerface, such as biochips, biosensors, bioseparators, and medical body implants.

Acknowledgment. We thank Japan Analytical Industry (Tokyo) for the fractionation of PHEMA by preparative GPC. This work was supported by Grant-in-Aids for Scientific Research, the Ministry of Education, Culture, Sports, Science and Technology, Japan (Grant-in-Aids 17002007 and 17205022).

References and Notes

(1) Ejaz, M.; Yamamoto, S.; Ohno, K.; Tsujii, Y.; Fukuda, T. *Macromolecules* **1998**, *31*, 5934.
(2) Huang, X.; Wirth, M. J. *Macromolecules* **1999**, *32*, 1694.
(3) Matyjaszewski, K.; Miller, P. J.; Shukla, N.; Immaraporn, B.; Gelman, A.; Luokala, B. B.; Siclovan, T. M.; Kickelbick, G.; Vallant, T.; Hoffmann, H.; Pakula, T. *Macromolecules* **1999**, *32*, 8716.
(4) Husseman, M.; Malmstrom, E. E.; McNamara, M.; Mate, M.; Mecerreyes, D.; Benoit, D. G.; Hedrick, J. L.; Mansky, P.; Huang, E.; Russell, T. P.; Hawker, C. J. *Macromolecules* **1999**, *32*, 1424.
(5) Kim, J.-B.; Bruening, M. L.; Baker, G. L. *J. Am. Chem. Soc.* **2000**, *122*, 7616.
(6) Zhao, B.; Brittain, W. J. *Prog. Polym. Sci.* **2000**, *25*, 677.

(7) Pyun, J.; Kowalewski, Y.; Matyjaszewski, K. *Macromol. Rapid Commun.* **2003**, *24*, 1043.
(8) Edmonsdon, S.; Osborne, V. L.; Huck, W. T. S. *Chem. Soc. Rev.* **2004**, *33*, 14.
(9) Tsujii, Y.; Ohno, K.; Yamamoto, S.; Goto, A.; Fukuda, T. *Adv. Polym. Sci.*, in press.
(10) (a) Yamamoto, S.; Ejaz, M.; Tsujii, Y.; Matsumoto, M.; Fukuda, T. *Macromolecules* **2000**, *33*, 5602. (b) Yamamoto, S.; Ejaz, M.; Tsujii, Y.; Fukuda, T. *Macromolecules* **2000**, *33*, 5608.
(11) Yamamoto, S.; Tsujii, Y.; Fukuda, T. *Macromolecules* **2002**, *35*, 6077.
(12) Urayama, K.; Yamamoto, S.; Tsujii, Y.; Fukuda, T.; Neher, D. *Macromolecules* **2000**, *35*, 9459.
(13) Yamamoto, S.; Tsujii, Y.; Fukuda, T.; Torikai, N.; Takeda, M. *KENS Rep.* **2001**−**2002**, *14*, 204.
(14) He, H.; Tsujii, Y.; Fukuda, T.; Nakanishi, K.; Ishizuka, N.; Minakuchi, H. *Polym. Prepr., Jpn. (Soc. Polym. Sci., Jpn.)* **2003**, *52*, 2961.
(15) Currie, E. P. K.; Norde, W.; Cohen Stuart, M. A. *Adv. Colloid Interface Sci.* **2003**, *100*−*102*, 205.
(16) (a) Jeon, S. I.; Lee, J. H.; Andrade, J. D.; Degennes, P. G. *J. Colloid Interface Sci.* **1991**, *142*, 149. (b) Jeon, S. I.; Andrade, J. D. *J. Colloid Interface Sci.* **1991**, *142*, 159.
(17) Halperin, A. *Langmuir* **1999**, *15*, 2525.
(18) Unsworth, L. D.; Sheardown, H.; Brash, J. L. *Langmuir* **2005**, *21*, 1036.
(19) Norde, W.; Gage, D. *Langmuir* **2004**, *20*, 4162.
(20) Kenausis, G. L.; Voros, J.; Elbert, D. L.; Huang, N.; Hofer, R.; Ruiz-Taylor, L.; Textor, M.; Hubbel, J. A.; Spencer, N. D. *J. Phys. Chem. B* **2000**, *104*, 3298.
(21) Efremove, N. V.; Boundurant, B.; O'Brien, D. F.; Leckband, D. E. *Biochemistry* **2000**, *39*, 3441.
(22) Xiano, D.; Zhang, H.; Wirth, M. *Langmuir* **2002**, *18*, 9971.
(23) Lee, S. B.; Koepsel, R. R.; Morley, S. W.; Matyjaszewski, K.; Sun, Y.; Russell, A. J. *Biomacromolecules* **2004**, *5*, 877.
(24) Ma, H.; Hyun, J.; Stiller, P.; Chikoti, *A. Adv. Mater.* **2004**, *16*, 338.
(25) Feng, W.; Brash, J. L.; Zhu, S. *J. Polym. Sci., Part A: Polym. Chem.* **2004**, *42*, 2931.
(26) Iwata, R.; Suk-In, P.; Hoven, V. P.; Takahara, A.; Akiyoshi, K.; Iwasaki, Y. *Biomacromolecules* **2004**, *5*, 2308.
(27) Feng, W.; Zhu, S.; Ishihara, K.; Brash, J. L. *Langumuir*, in press.
(28) Montheard, J. P.; Chatzopoulos, M.; Chappard, D. *J. Macromol. Sci., Rev. Macromol. Chem. Phys.* **1992**, *C32*, 1.
(29) (a) Ishihara, K.; Aragaki, R.; Ueda, T.; Watanabe, A.; Nakabayashi, N. *J. Biomed. Mater. Res.* **1990**, *24*, 1069. (b) Ishihara, K.; Ziats, N. P.; Tierney, B. P.; Nakabayashi, N.; Anderson, J. M. *J. Biomed. Mater. Res.* **1991**, *25*, 1397.
(30) Sawada, S.; Sakaki, S.; Iwasaki, Y.; Nakabayashi, N.; Ishihara, K. *J. Biomed. Mater. Res.* **2003**, *3*, 411.
(31) Tanaka, M.; Motomura, T.; Kawada, M.; Anzai, T.; Kasori, Y.; Shiroya, T.; Shimura, K.; Onishi, M.; Mochizuki, A. *Biomaterials* **2000**, *21*, 1471.
(32) Tanaka, M.; Mochizuki, A.; Motomura, T.; Shimura, K.; Onishi, M.; Okahata, Y. *Colloids Surf., A* **2001**, *193*, 145.
(33) Beers, L. K.; Boo, S.; Gaynor, S. G.; Matyjaszewski, K. *Macromolecules* **1999**, *32*, 5772.
(34) Ohno, K.; Morinaga, T.; Koh, K.; Tsujii, Y.; Fukuda, T. *Macromolecules* **2005**, *38*, 2137.
(35) Robinson, K. L.; Khan, M. A.; de Paz Banez, M. V.; Wang, X. S.; Armes, S. P. *Macromolecules* **2001**, *34*, 3155.
(36) Sauerbrey, G. *Z. Phys.* **1959**, *155*, 206.
(37) Jones, D. M.; Huck, W. T. S. *Adv. Mater.* **2001**, *13*, 1256.
(38) Zhou, F.; Liu, W.; Hao, J.; Chen, M.; Liu, W.; Sun, D. C. *Chem. Lett.* **2004**, *33*, 602.
(39) Huang, W.; Kim, J.-B.; Bruening, M. L.; Baker, G. L. *Macromolecules* **2002**, *35*, 1175.
(40) Baszkin, A.; Lyman, D. J. *J. Biomed. Mater. Res.* **1980**, *14*, 393.
(41) Suttiprasit, P.; Krisdhasima, V.; Mcguire, J. *J. Colloid Interface Sci.* **1992**, *154*, 316.
(42) Carter, D. C.; He, X.-M. *Science* **1990**, *249*, 302.
(43) Hook, F.; Rodahl, M.; Brzezinski, P.; Kasemo, B. *Langmuir* **1998**, *14*, 729.
(44) Asolphi, U.; Kulicke, W.-M. *Polymer* **1997**, *38*, 1513.
(45) Liy, J. H.-Y.; Brant, D. A.; Kitamura, S.; Kajiwara, K.; Mimura, M. *Macromolecules* **1999**, *32*, 8611.
(46) Tsuruta, T. *Adv. Polym. Sci.* **1996**, *126*, 1.
(47) (a) Fujimoto, K.; Inoue, H.; Ikada, Y. *J. Biomed. Mater. Res.* **1993**, *27*, 1559. (b) Fujimoto, K.; Tadokoro, H.; Ueda, Y.; Ikada, Y. *Biomaterials* **1993**, *14*, 442.
(48) Nojiri, C.; Nakahama, S.; Senshu, K.; Okano, T.; Kawagoishi, N.; Kido, T.; Sakai, K.; Koyanagi, H.; Akutsu, T. *ASAIO J.* **1993**, *39*, 322.
(49) Nojiri, C.; Senshu, K.; Okano, T. *Artif. Organs* **1995**, *19*, 32.
(50) Senshu, K.; Yamashita, S.; Ito, M.; Hirao, A.; Nakahama, S. *Langmuir* **1995**, *11*, 2293.
(51) Senshu, K.; Yamashita, S.; Mori, H.; Ito, M.; Hirao, A.; Nakahama, S. *Langmuir* **1999**, *15*, 1754.
(52) Senshu, K.; Kobayashi, M.; Ikawa, N.; Yamashita, S.; Hirao, A.; Nakahama, S. *Langmuir* **1999**, *15*, 1763.

MA0520242